Innovative Polyurethane Foam from Agro-Industrial and Petrochemical Waste: A Sustainable Solution for Adsorbing Organic Pollutants in Natural Waters

Marys Lene Braga Almeida[a]* ⓘ *, Bruna Nitzsche Morato[a], Verenna Santos Guedes[a], Eliane Ayres[b],*

Patrícia Alves Saliba[a], Jacqueline Maria Flor[c], Andreia Bicalho Henriques[d] ⓘ *, Marcelo Libânio[e]* ⓘ *,*

Rodrigo Lambert Oréfice[f] ⓘ

[a]*Universidade Federal de Minas Gerais, Departamento de Engenharia de Materiais e Construção, 31270901, Belo Horizonte, MG, Brasil.*
[b]*Universidade do Estado de Minas Gerais, Escola de Design, Departamento de Investigação Tecnológica, 30140-091, Belo Horizonte, MG, Brasil.*
[c]*Universidade Federal de Minas Gerais, Departamento de Engenharia de Estruturas, 31270901, Belo Horizonte, MG, Brasil.*
[d]*Universidade Federal de Minas Gerais, Departamento de Engenharia de Minas, 31270901, Belo Horizonte, MG, Brasil.*
[e]*Universidade Federal de Minas Gerais, Departamento de Engenharia Sanitária e Ambiental, 31270901, Belo Horizonte, MG, Brasil.*
[f]*Universidade Federal de Minas Gerais, Departamento de Engenharia Metalúrgica e de Materiais, 31270901, Belo Horizonte, MG, Brasil.*

Fluid catalytic cracking is essential in petroleum refining but generates harmful silica-rich spent catalysts (CR). Agricultural waste, like burned rice husks, produces high-silica ashes (RHA). Both CR and RHA are promising waste-derived adsorbents. Polyurethane foams (PUFs) are ideal for adsorbing pesticides in water due to their multiple binding sites, making them effective supports for retaining various pesticide classes. Bio-based PUF was synthesized and incorporated with 50% CR or RHA by polyol mass. The sorbents were analyzed using X-ray diffraction, scanning electron microscopy, microtomography, thermogravimetric analysis, infrared spectroscopy, and contact angle. Effectiveness of the adsorbents in aqueous systems was evaluated by adsorption efficiency at different pHs (2.0, 7.0, and 12.0) using pesticides mancozeb, glyphosate, and 2,4-dichlorophenoxyacetic acid. In the experiment with mancozeb after 24 hours at pH 2.0 and a concentration of 300 mg L^{-1}, pure PUF-REF obtained an adsorption efficiency of 85% (38.60 mg/g). In the same experiment, PUF loaded with CR achieved 98% (45.98 mg/g) removal of pesticide, while PUF loaded with RHA obtained adsorption efficiency of 62.5% (29.87 mg/g). This work examines the use of petrochemical and agro-industrial wastes as adsorbents for removing organic contaminants from natural waters, highlighting their potential to enhance sustainability and circular economy practices.

Keywords: *Polyurethane Foam, Alternative Adsorbents, Petroleum Catalyst Residue, Rice Husk Ash, Pesticides.*

1. Introduction

Pesticides are compounds used to kill pests (insects, rodents and fungi) and weeds whose uncontrolled use can cause serious problems for non-target organisms, such as water contamination[1]. In aquatic systems, this contamination occurs through crop runoff, becoming a global health concern, especially in Brazil, a country considered to be one of the largest consumers of pesticides in the world. Approximately 80% of the pesticides authorized for sale are banned in at least three countries of the Organization for Economic Cooperation and Development (OECD) and the European Community[2].

The rapid urbanization and industrialization have severely damaged global water resources with organic and inorganic pollutants, as continuous discharge of industrial, municipal, and farm runoff effluents contaminates groundwater, threatening both healthy ecosystems[3-5]. It is estimated that 10–20 million deaths annually due to waterborne diseases, including over 200 million deaths worldwide each year, with around 5,000–6,000 children dying daily from conditions like diarrhea, and more than 0.78 billion people lacking access to safe water sources globally[6].

Poor basic sanitation conditions pose a great risk to human health, since pesticides are not removed by conventional treatment, despite being monitored in treatment plants[7]. Due to this, excessive levels of organic chemicals, such as pesticides, have been detected in drinking water[3].

---

*e-mail: marys@demc.ufmg.br

In Brazil, the most widely sold pesticides, such as glyphosate, 2,4-D (2,4-dichlorophenoxyacetic acid) and mancozeb, are linked to various health problems, including possible cases of cancer[8]. Glyphosate, a widespread pesticide, has been considered a probable carcinogen by the International Agency for Research on Cancer (IARC), associated with non-Hodgkin's lymphoma and reproductive toxicity[9-11]. 2,4-D is also classified as a possible human carcinogen by the IARC, while mancozeb, classified as a carcinogen by the European Union, is associated with respiratory and neurological risks[12-14].

Common water treatment technologies such as ion-exchange, adsorption, chemical precipitation, membrane filtration, oxidation, and photocatalysis have shown that hazardous chemicals are persistent and challenging to remove[5]; Therefore, a reliable, cost-effective, and eco-friendly solution is needed to remove these substances and protect human health and the environment[15].

The adsorption process refers to the attachment of a substance to a surface through molecular attraction, which can occur via physical adsorption, chemical adsorption, or a combination of both[16]. Physical adsorption (physisorption) involves the adherence of molecules or atoms to a surface through weak intermolecular forces—primarily van der Waals interactions. Already the chemical adsorption (chemisorption) involves stronger interactions, typically through chemical bonds, such as covalent bonds, or functional groups on the surface, such as carboxyl or hydroxyl groups. The degree of chemical bonding depends on the number of available functional groups and the surface area accessible for adsorption[5]. Overall, adsorption is generally regarded as a viable and highly efficient process[17], though it can sometimes be high cost. Estimates suggest that the cost of using adsorption technology for water treatment ranges from 5.0 to 200 US dollars per cubic meter of water[18]. Because of that, the first step towards an efficient adsorption process is to choose an easily obtainable adsorbent with high selectivity, low cost and removal capacity.

Activated carbon is the most commonly used adsorbent for removing various pollutants from water[19,20]. This material is known for its advantageous stability and porosity for the adsorption process and can be produced from carbon sources using carbonization and activation processes. However, the high cost and challenging acquisition of raw materials limit their use as adsorbents, while the dominance of micropores in activated carbon restricts the diffusion and accessibility of organic pollutants, reducing its adsorption capacity and limiting its use as an adsorbent[21].

In this context, researchers have looked to unconventional materials such as agricultural residues (rice shells, sewage sludge compost, *Moringa oleifera*, *Alcaligenes faecalis* and sunflower seeds)[22-24] to adsorb organic contaminants in water. Other reported alternatives are activated carbon compost with zinc and magnesium compost[25], biochars[26], graphene-based materials[27-29], iron composite nanoparticles[30,31], montmorillonite and bauxite[32], zeolites[33,34], titanium oxide nanoparticles[35] and polyurethane foams (PUF)[36].

PU-based materials have chemical and physical properties suitable for the adsorption of aqueous contaminants, with high adsorption capacity, chemical and thermal resistance, low cost, easy to obtain and the ability to retain various types of microcontaminants. The different functional groups in their structures - ether, ester, urea, amides and urethane groups - and the possibility of adjusting the geometric structure and size of their cells and pores, and of chemically modifying their surface, give the foams important properties for use as adsorbents[1].

Polyurethane foams are materials that can be manufactured with relatively low energy requirements and minimal capital investment in equipment. They are produced by reacting isocyanates with polyols, usually in the presence of a catalyst or ultraviolet (UV) light[37]. Most polyurethane foams are prepared from raw materials obtained from petrochemical industries; however, the petrochemical raw material is not renewable, and its production and use result in a serious greenhouse effect. Therefore, foams produced solely from petrochemical materials can no longer meet the needs of long-term low-carbon development strategy[38].

Although traditionally derived from petroleum, polyols have been replaced by renewable alternatives, such as vegetable oils, due to high energy consumption and environmental concerns. Rich in reactive functional groups, these oils can be converted into polyols by processes such as epoxidation, ozonolysis and transesterification, enabling their partial application in the production of PUs. The growing global demand for PUs reinforces the importance of recycling methods, which include chemical and mechanical processes, energy recovery and reuse[36,39], with environmental and economic benefits. An interesting property of PU foams based on plant-based polyols is the possibility of their regeneration and reuse[1].

Incorporating fillers into polymer foams enhances physical properties like mechanical and thermal characteristics, modifies polymer structures, acts as nucleants and promotes cell nucleation during foaming processes. Furthermore, PUF has enough dimensional stability, which makes this foam an excellent choice for developing a porous support whereupon adsorbent particles can be attached[40].

The performance of fillers in wastewater treatment affects energy consumption, efficiency, and stability. Traditional fillers include inorganic, organic, and synthetic polymers, but polyurethane sponge (PU) fillers have recently gained attention for their low cost, high porosity, and effectiveness in supporting microorganism growth and removing organics and nutrients[41].

The petrochemical and agro-industrial sectors generate residue with a high potential for reuse. Among these residues, petroleum catalyst (CR) and rice husk ash (RHA) stand out as materials with promising applications in the area of adsorption, offering opportunities for their reuse[1,42].

CR is a porous particulate material, with pores of approximately 4 nm, composed mainly of SiO_2 (55.7% by weight) and Al_2O_3 (37.2% by weight)[36]. RHA is a particulate material with irregular shapes and microporous cellular structures, with the presence of cristobalite and a silica content of over 70%[43]. The high silica content is due to the burning of this material, generating SiO_2[36].

With this in mind, this work aims to evaluate the removal of the pesticide's glyphosate, 2,4-D and mancozeb from aqueous solutions with different pH ranges using polyurethane foams and composites. This study offers an innovative solution for removing pesticides from aqueous solutions while also proposing an environmentally friendly and cost-effective method for preparing PU composites.

Innovative Polyurethane Foam from Agro-Industrial and Petrochemical Waste: A Sustainable Solution for Adsorbing Organic Pollutants in Natural Waters

3

In this way, the aim is to improve water quality by reducing pesticides, as set out in the Sustainable Development Goals of the UN 2030 Agenda[44].

2. Materials and Methods

2.1. Materials

The petroleum catalyst residue (CR) was kindly provided by REGAP, PETROBRAS, located in Betim-MG, Brazil. The rice husk ash (RHA) was supplied by Indiana Distribuição (Embu das Artes – SP, Brazil), and is commercialized as Silcca Nobre SBI®. Biopol® 411, a polyol derived from castor oil with hydroxyl number of 294 mg KOH g^{-1} and functionality 2.7, is produced by Poly-Urethane (Ibirité-MG, Brazil). Polymeric methylene diphenyldiisocyanate (pMDI), molar mass of 349.9 g mol^{-1} and average functionality 2.6, is imported from Asian countries by Poly-Urethane and sold as Biopol® ISO. The catalyst Tin(II) octoate, with trade name Liocat® 29 (TIN) is provided by Miracema-Nuodex (Campinas-SP, Brazil). Tegostab® B 8135, silicone with high stabilizing potency, by Evonik (distribution center in Guarulhos-SP, Brazil). From Sigma-Aldrich are: polypropylene glycol-PPG 2000 (81380), mancozeb (45553), glyphosate (45521) and 2,4-D (2,4-dichlorophenoxyacetic acid) (49083).

2.2. Polyurethane foam and composites synthesis

The pure polyurethane foam (PUF), used as reference (PUF-REF), was synthesized using the "one-shot" process at room temperature (25 ± 3°C), as established by Almeida et al.[1] and shown in Table 1 and Figure 1. The synthesis involved mixing 11.25g of Biopol 411, 1.25g of PPG 2000, 0.40g of deionized water, 0.025g of TIN and 0.10g of Tegostab® B 8135 at a speed of 1000 rpm for 2 min. Then, 16.74g of MDI was added and stirring for a further 30 sec. The resulting composition was left to stand for 48 h at room temperature.

The PUF-CR and PUF-RHA polyurethane composites (Figure 1) were produced in the same way, by incorporating 50% CR or RHA (as for the total polyol mass) along with the polyols.

2.3. Characterizations

2.3.1. BET surface area

The BET specific surface area of CR and RHA was analyzed using Quantachrome equipment, model Nova Station A' (Anton Paar GmbH, USA). The samples were analyzed in a nitrogen atmosphere (adsorption-desorption isotherms at 77 K), using multi-point measurement, with relative pressures (P/P0) ranging from 0.01 to 0.99.

Table 1. Foam formulation.

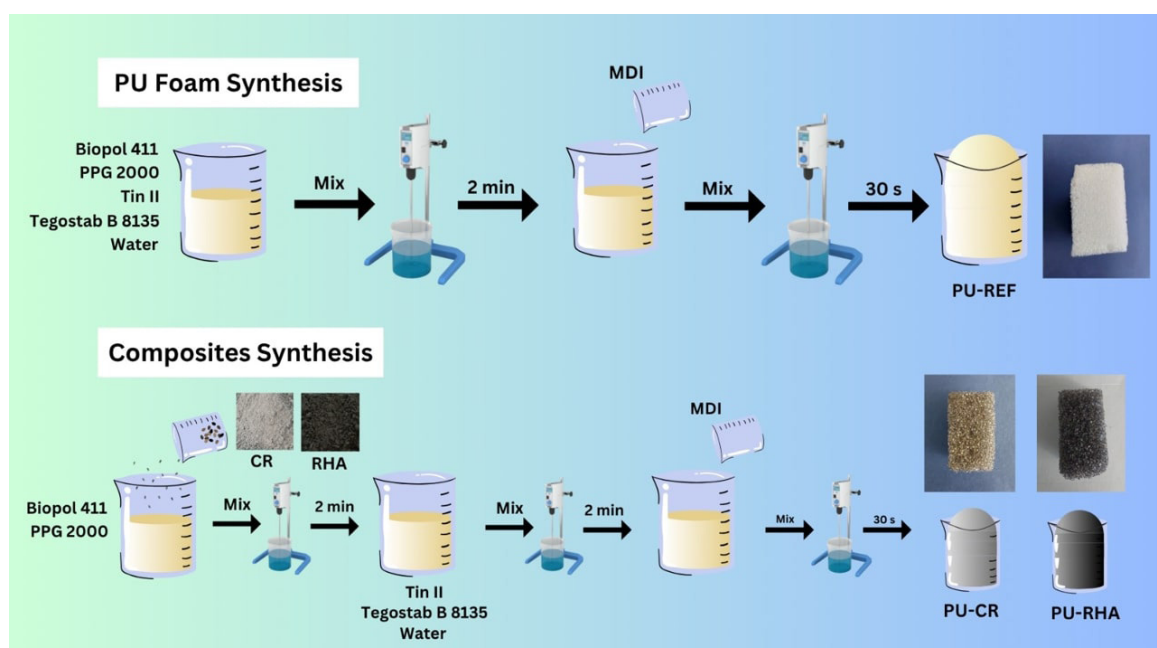| Foam Sample	Residue CR/RHA	Polyol PPG 2000	Polyol Biopol® 411	Catalyst TIN	Silicone Tegostab	Expander Deionized Water	Isocyanate MDI
PUF- REF	0.00/0.00	1.25	11.25	0.025	0.10	0.40	16.74
PUF-CR	6.25/0.00	1.25	11.25	0.025	0.10	0.40	16.74
PUF-RHA	0.00/6.25	1.25	11.25	0.025	0.10	0.40	16.74

*units in grams.

Figure 1. Schematic representation of PUFs formation process.

The samples were previously prepared by degassing at 100 °C for 48 h. The Barrett, Joyner and Halenda (BJH) and non-local density functional theory (NLDFT) methods were used to determine the average pore diameter and volume.

2.3.2. X-ray diffraction

The X-ray diffraction patterns of CR and RHA were obtained using an X-ray diffractometer (PANalytical X'Pert, Empyrean, Netherlands) equipped with a Cu tube (CuKα radiation, λ = 6 Å) and a graphite crystal monochromator, operating at 40 kV and 40 mA. The scan was carried out at a rate of 0.06 s^{-1} for 2θ ranging from 3 to 90°.

2.3.3. Scanning electron microscopy (SEM)

The fractured surfaces of the polyurethane foam and its composites were examined using scanning electron microscopy (SEM) (FEI, model INSPECTTM S50) coupled with energy dispersive X-ray spectroscopy (EDX, EDAX GENESIS, Czech Republic). The SEM samples (1 × 1 cm^2) were immersed in liquid nitrogen, fractured and coated with gold using a sputter coater (SPI Sputter Coater, SPI Supplies, PA, USA). Fracturing the samples exposed the cellular structure of the polymer. Before analysis, the samples were coated with a thin layer of gold by sputtering at a low deposition rate. The images were captured using secondary electrons with an accelerating voltage of 15 kV.

2.3.4. X-ray microtomography

Details of the morphologies of the polyurethane foam and composites were obtained by X-ray microtomography (Skyscan 1174, Aartselaar, Belgium), using an X-ray source voltage of 35 kV, current of 800 A, and a three-dimensional (3D) spatial resolution of 8.05 μm. Two-dimensional images of the positioned samples were acquired using unfiltered X-ray beams at 0.7° intervals, followed by software-assisted reconstruction (NRecon v.1.6.9.18, Skyscan, Bruker microCT, Belgium). 3D models were built using CTAN v.1.15.4.0 software (Bruker microCT, Belgium), and visualization of 3D images of bulk materials was carried out using CTVol v.2.3.1.0 (Skyscan, Bruker microCT, Belgium).

2.3.5. Thermogravimetric analysis (TGA)

Thermogravimetric analysis (TGA) of the residues, polyurethane foam and composites was carried out by weighing 8.0±1 mg of the samples using Seiko-SII Nanotechnology Inc., Japan, model Exstar 7200, under a nitrogen atmosphere (with a flow rate of 30 cm^3 min^{-1}). The samples were heated in a platinum crucible from 25 °C to 800 °C, at a heating rate of 10 °C min^{-1}.

2.3.6. Fourier transform infrared spectroscopy (FTIR)

The chemical groups of the residues, the polyurethane foam and the composites were analyzed using Fourier Transform Infrared Spectroscopy (FTIR), using a Thermo Scientific Nicolet TM 6700 Gold spectrometer with the Attenuated Total Reflection (ATR) technique. The samples were pressed against a ZnSe crystal, and the analysis covered the 4500-450 cm^{-1} range, with 32 scans and a resolution of 4 cm^{-1}.

2.3.7. Contact angle

The hydrophobicity of the PUF-REF, PUF-CR and PUF-RHA was investigated by measuring the contact angle. The measurements were carried out by depositing a drop of deionized water, using a 1 mL syringe, on the surface of the samples at room temperature (25±3°C).

2.4. Pesticides adsorption

The polyurethane foams (PUFs) were cut into approximately uniform cubes, each with a volume of about 0.8 cm^3. A pre-established fixed mass of adsorbent was used in all adsorption assays to ensure representativeness and allow for comparison of the results. The foam cubes were individually weighed and directly added to the solutions for each experimental condition.

In 100 mL amber glasses, 20 mL of the aqueous solution of 50 and 300 mg L^{-1} of the pesticide was poured into deionized water at pH 7. Subsequently, 120 mg of the each foam were added to the bottles. These vessels were subjected to mechanical agitation (Mod 786, Fisatom) at 150 rpm for 24 h, followed by filtration Millex-HV Syringe Filter with 0.45 μm membrane (Sigma-Aldrich - SLHVR33RS). The filtrate was then analyzed by UV-Vis at 193 nm for glyphosate, 279 nm GIR for mancozeb and 283 nm for 2,4-D[45-47]. The foams were submitted to the same process with 50 and 300 mg L^{-1} solutions at pH 2 and 12. The amounts of glyphosate and mancozeb were determined in aqueous solution using an ultraviolet-visible (UV-Vis) spectrophotometer (UV-2600, Shimadzu Corporation), using a quartz cuvette (Kasvi) over the wavelength range 185 to 400 nm. As for 2,4-D, it was evaluated in a 1:1 v/v methanol: water solution[1]. Figure 2 illustrates the absorption method for pesticide removal by the foams.

A control experiment was performed under the same conditions as the sorption tests — identical contaminant concentrations, pH, and stirring time — but in the absence of adsorbents (PUF-REF, PUF-CR, and PUF-RHA). The prepared aqueous solutions were subjected to mechanical stirring at 150 rpm for 24 hours, followed by filtration using a Millex-HV syringe filter with a 0.45 μm membrane (Sigma-Aldrich – SLHVR33RS). Filtrates from each solution were then analyzed by UV-Vis spectrophotometry at the following wavelengths: 193 nm for glyphosate, 279 nm for mancozeb, and 283 nm for 2,4-D.

All assays were performed in triplicate. Equations 1 and 2 were applied to determine the adsorption efficiency (E%) and adsorption capacity (Qe) (mg of adsorbate/g adsorbent), respectively.

$$\%E = \frac{(Co - Ce)}{Co} x\ 100 \tag{1}$$

$$Qe = (Co - Ce) x \frac{v}{m} \tag{2}$$

where Co and Ce are the initial in the solution and the final contaminant concentration at any given time (mg. L^{-1}), respectively, V is the volume of solution (L) and m is the mass of adsorbent (mg).
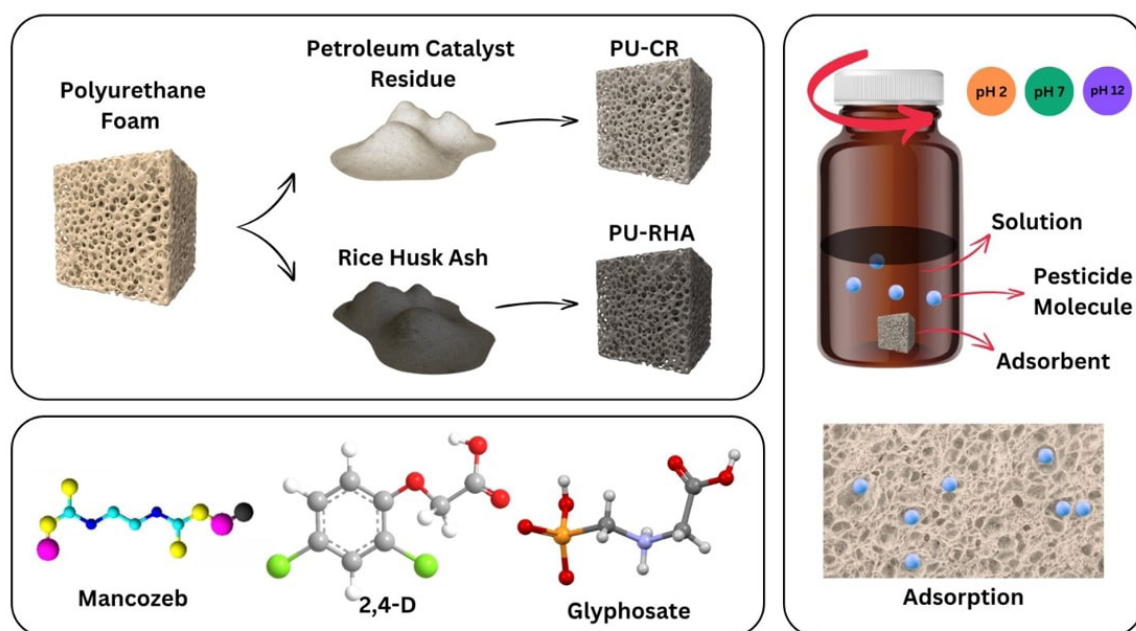
Innovative Polyurethane Foam from Agro-Industrial and Petrochemical Waste: A Sustainable Solution for
Adsorbing Organic Pollutants in Natural Waters

5

Figure 2. Illustration of the absorption method for pesticide removal by the foams.

Table 2. Surface area and porosity of RHA and CR.

SAMPLE	S_{BET}	$V_{(p)}$	$D_{(average)}$
	(m²/g)	(cm³/g)	(nm)
RHA	5.580 ± 1.200	0.012 ± 0.006	0.160 ± 0.680
CR	150.000 ± 15.000	0.160 ± 0.016	4.200 ± 0.420

*Specific surface area (S_{BET}), Total pore volume (V_p) and Mean pore diameter (D).

2.5. Contact time

The contact time between sorbents and pesticide solution was evaluated to determine the kinetic of adsorption. The experiment was conducted for 44h in a system with a pH value of 2 and a Mancozeb concentration of 300mg/L.

3. Results and Discussion

3.1. Characterization of petroleum catalyst residues and rice husk ash

The specific surface area of RHA and CR was evaluated, since this parameter is relevant as a morphological characteristic associated with adsorbent materials: increasing the area increases the number of sites available for adsorption[48]. The specific surface area of RHA and CR was found to be 5.58 m²g⁻¹ and 150 m²g⁻¹, respectively. The value concerned to RHA was lower than those found by some authors, for example, 32.6 m²g⁻¹ and 65.36 m²g⁻¹[49,50]. Probably, the variety of rice husks gives rise to ashes with diverse specific surface areas[42]. In the case of CR, the value of specific surface area is in agreement with other authors[36,51,52].

Porous materials can be classified in terms of their structure as microporous, mesoporous and macroporous, depends on their pore diameter. Pores smaller than 2.0 nm,

pores between 2.0 nm and 50 nm and pores larger than 50 nm, respectively[48]. Therefore, RHA with pore diameter of 0.16 nm has a microporous structure and CR with pore diameter of 4.20 nm has a mesoporous structure. Table 2 summarizes the parameters determined for the porous residues. In addition, according to the toxicity characteristics leaching procedure, CR is classified as non-hazardous residue and can be categorized as general industrial residue[1].

X-ray diffraction analysis of the particulate materials (Figure 3) showed that both have well-defined peaks. In the analysis of the X-ray diffraction pattern of CR, as discussed by researchers[36], it is noticeable that there is a broad peak between 6.22° and 30°, which is indicative of the presence of faujasite-type zeolite. Zeolites are highly effective and cost-efficient adsorbents for removing wastewater pollutants, thanks to their excellent ion-exchange capacity, large surface areas, and cage-like structures[18]. The peak at 67.17° is attributed to the quartz (SiO_2) present in the CR structure. Other peaks are attributed to cristobalite, mullite and quartz[1,36]. The RHA diffraction pattern shows an intense peak around 22°, which typically indicates the formation of amorphous silica, as well as other small peaks at 36°, 65° and 78°, suggesting a pattern compatible with silica in the form of cristobalite, formed during the combustion of RHA[53,54].
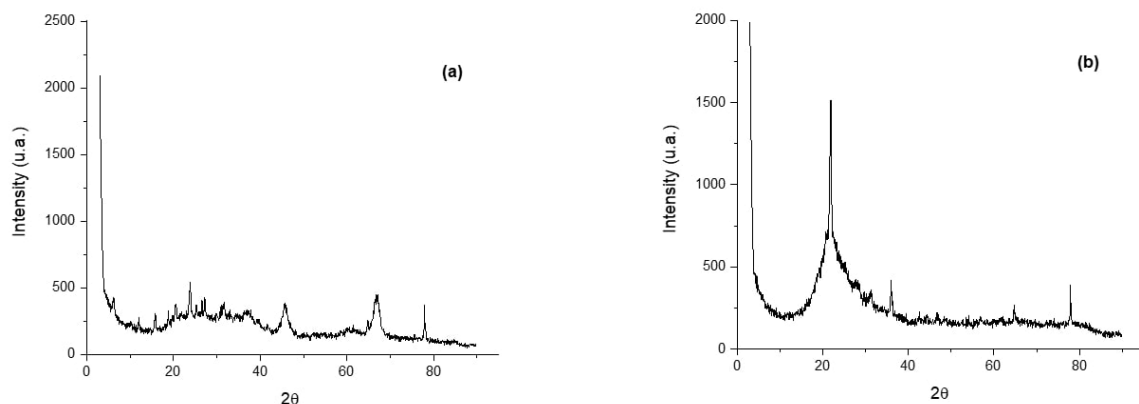
Figure 3. X-ray diffraction analysis of: (a) CR and (b) RHA.

Thermal analysis of RHA and CR (Figure 4) revealed a reduced loss of mass when the material was heated, indicating the thermal stability of these materials. Both materials show an initial loss of mass (up to 200°C) related to water adsorbed on the surface of the particles. After this temperature, burning and decomposition of the inorganic material occurs[53].

Chemical analysis of the adsorbents using the FTIR technique (Figure 5) indicated the presence of intense bands around 1069 cm^{-1} and 1086 cm^{-1} for CR and RHA, respectively. These bands are characteristic of the Si-O-Si clusters that make up the structure of silica (SiO_2) and which appear in different forms in particulate materials, as indicated in the XRD analysis (Figure 3)[42,54,55]. In addition, FTIR analysis confirms the inorganic nature of the particulate adsorbents, due to the absence of bands related to organic groupings.

3.2. Characterization of foam and composites

Figure 6 illustrates the visual differences between foams and composites. In Figure 6a, the pure polyurethane foam shows a light-colored material and the PU-CR composite, Figure 6c, shows a more grayish color due to the incorporation of CR. PU-RHA (Figure 6e), on the other hand, has an even darker color, due to the color of the RHA being darker than that of the CR.

The SEM image reveals a three-dimensional, interconnected porous structure with abundant macropores formed, promoting rapid diffusion, buffering, and storage of pollutant molecules for optimal utilization of the porous network[21]. The cell structure of foam plays a crucial role in determining its mechanical properties, sound absorption, and overall performance[38]. The SEM images of the adsorbents (Figures 6b, c, f) show that the addition of RHA and CR to the foams practically did not alter the cellular structure and integrity of the foams, with open and interconnected pores, as well as pores of different sizes, which favors mass transport and contact between contaminant and adsorbent, favoring their removal process in aqueous systems[1,40].

The addition of RHA and CR to the polyurethane matrix (indicated by the white arrows) shows an adequate dispersion of the particulate material in the polymer matrix, although CR has some agglomerated particles. The particles attached onto
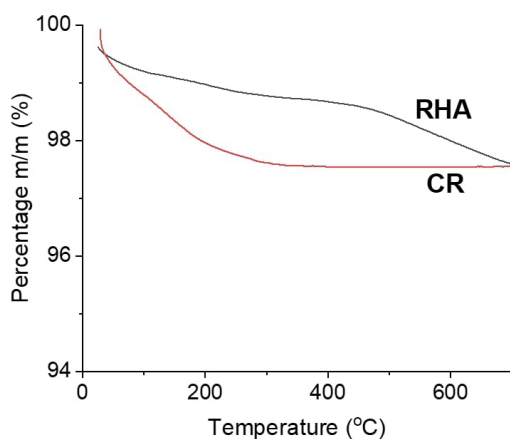

Figure 4. Thermogravimetric analysis of: CR and RHA.
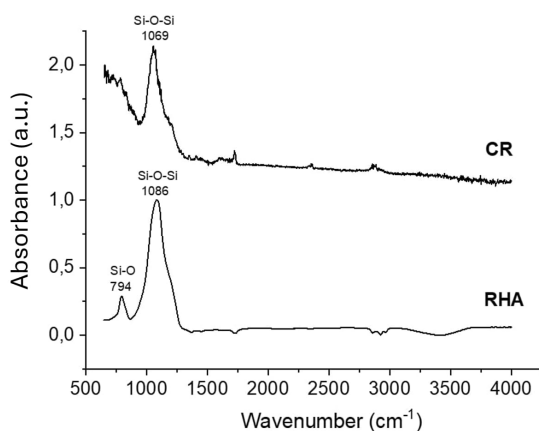

Figure 5. Fourier transform infrared spectroscopy spectra of: CR and RHA.

its skeleton surface and the particles are evenly distributed, resulting in an increase in the roughness, compared with that of PU foam, characteristic that is satisfactory for increasing the polymer's adsorption efficiency[40,56].

Innovative Polyurethane Foam from Agro-Industrial and Petrochemical Waste: A Sustainable Solution for
Adsorbing Organic Pollutants in Natural Waters

7

A more detailed analysis of foam porosity, performed using X-ray microtomography (Micro-CT, Figure 7), revealed preserved interconnectivity between pores. The total porosity of the pure foam was 96.77%, with slight variations observed for PU-CR (93.83%) and PU-RHA (95.12%). However, the maximum pore size decreased after incorporating RHA (Figure 7d), and decreased even further with the addition of CR (Figure 7f). The average pore size of the pure foam was 656 µm, increasing to 806 µm in PU-RHA and decreasing to 294 µm in PU-CR.
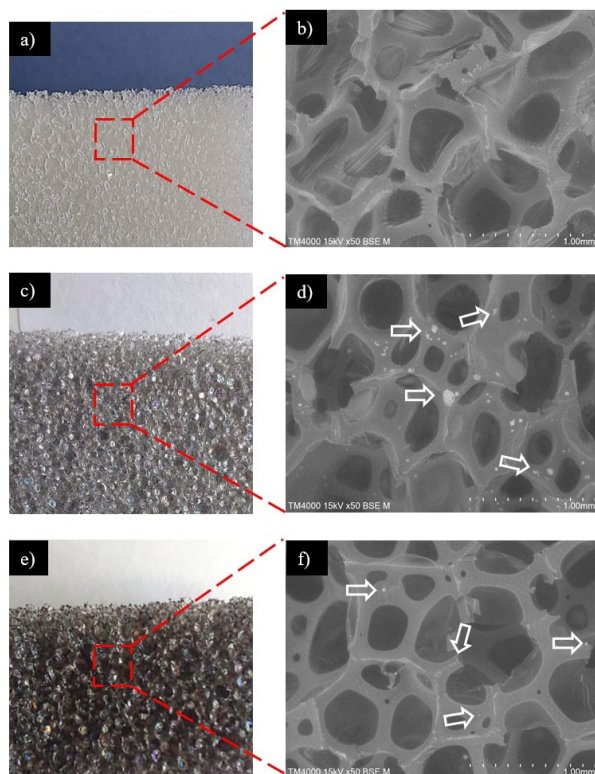

Figure 6. Images of: (a) PU-REF, (c) PU-CR, (e) PU-RHA. Scanning Electron Microscopy of: (b) PU-REF 50x, (d) PU-CR 50X, (f) PU-RHA 50X.
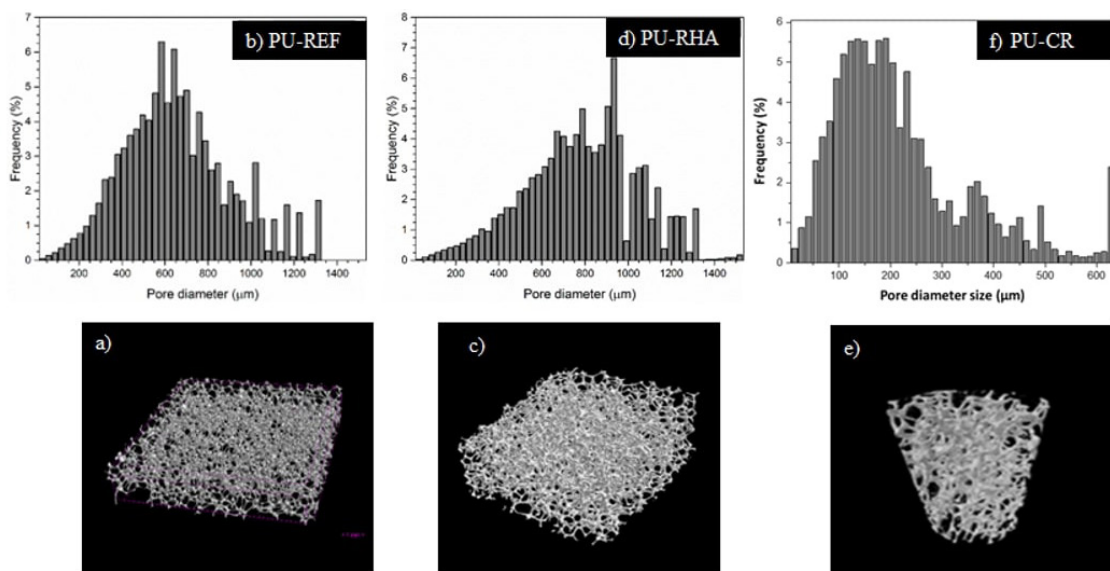

Figure 7. X-ray microtomography of: (a) PU-REF, (c) PU-RHA, (e) PU-CR. Total porosity distribution of: (b) PU-REF, (d) PU-RHA, (f) PU-CR.

A progressive reduction in the number of open pores was observed with the incorporation of residues. Smaller pores, as seen in PU-CR (294 µm), can enhance adsorption capacity by increasing surface area and promoting stronger interactions. In contrast, larger pores, such as those in PU-RHA (806 µm), facilitate diffusion but offer lower surface area and weaker interactions. The PU-REF foam, with an average pore size of 656 µm, showed intermediate adsorption performance.

Figure 8 shows the thermogravimetry analysis of the foam and composites with the incorporation of residues. The curves show similarities in thermal decomposition, with three stages. A first stage of mass loss was observed around 275°C, which can be related to the degradation of the rigid urethane and urea segments belonging to the foam. The second stage occurs at around 375°C and can be attributed to the degradation of soft segments of the foam's polymer chain. The third stage of decomposition, around 455°C,
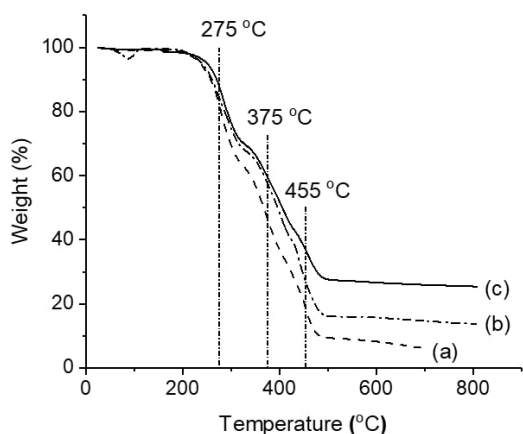
is associated with the decomposition of fragments generated during the second stage. Above 700°C, the decomposition of pure polyurethane foam produces no residue. In the case of the composites, as expected, there is residue, since RHA and CR are relatively stable against thermal decomposition up to the temperature evaluated. It is known that silica-based adsorbents are chemically and thermally stable[18,57]. The results of this work are in line with studies carried out by Almeida et al.[1], Pereira et al.[42], Kahlerras et al.[58] and Lu et al.[59]; and show that incorporating CR and RHA significantly improves the thermal stability of the composite foam, similar to what Xu at al[56]. observed.

The FTIR spectra obtained for the CR and RHA (Figure 9) showed the presence of typical bands of silica. The bands at 1089 cm^{-1} and 1026 cm^{-1} are attributed to the asymmetrical stretching vibration of Si-O-Si bond of the structural siloxane groups[60]. The Si-O-Si clusters that make up the structure of silica (SiO_2) appear in different forms in particulate materials, as indicated in the XRD analysis (Figure 3)[42,54,55]. The band around 800 cm^{-1} in both spectra is assigned to the symmetric stretching vibration of the Si-O bond[60].

Researchers defined an index $\omega = 100 \times (I_{800}/I_{1100})$ as a measurement of the three-dimensional organization of silica. According to them, when comparing two types of silica, higher value of ω indicates a well-organized silica network. Herein, CR and RHA did not present significant difference in the ω values[61].

The main FTIR bands of the polyurethane are given in Table 3[38,42,56,60-62]. The predominance of polyurethane bands are clear in both spectra of PUF-REF and composites (Figure 10).

Compared with PUF-REF spectrum, the composite spectra showed very slight differences. For example, the band relating to isocyanate groups -NCO (2270 cm^{-1}) in the spectra of the composites remained unchanged. According to researchers[42], the incomplete reaction during foam synthesis is probably due to the increase in viscosity of the reaction medium when the particulate adsorbent is added.
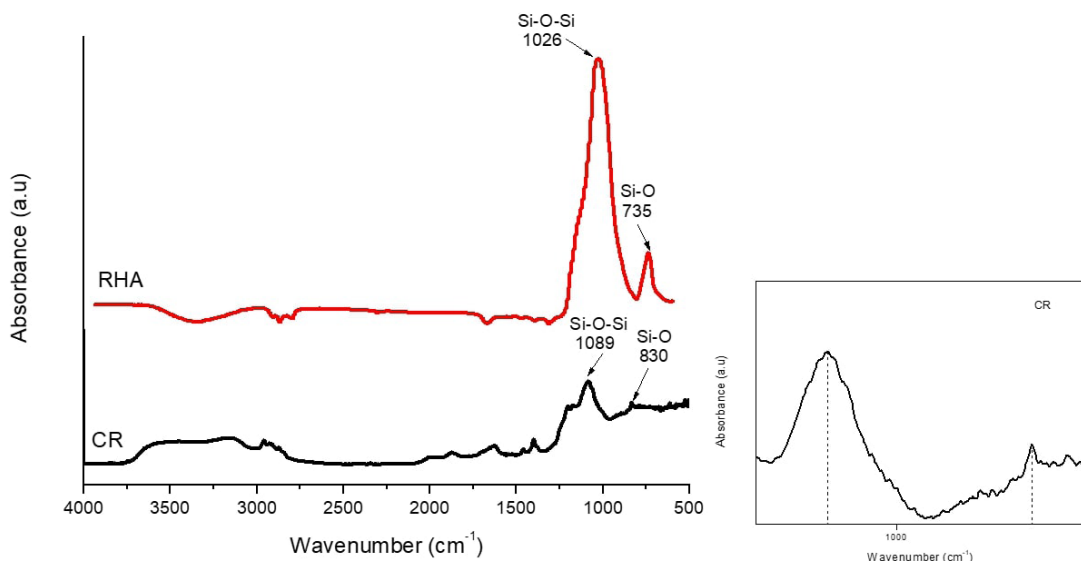

Figure 8. TGA curves of : a) PU-REF, b) PU-RHA and c) PU-CR.

Figure 9. Fourier transform infrared spectroscopy spectra of: CR and RHA. The inset shows the enlarged region of CR spectrum.

Innovative Polyurethane Foam from Agro-Industrial and Petrochemical Waste: A Sustainable Solution for
Adsorbing Organic Pollutants in Natural Waters

9

Herein, this situation was not observed due to the high reactivity of the reagents, as demonstrated by the PUF-REF spectrum with the low intensity band at 2270 cm^{-1}. The evident band at 1685 cm^{-1} in PUF-REF spectrum, typically attributed to urea C=O, was shifted towards higher frequencies region (1700 cm^{-1}) in PUF-RHA spectrum. This might indicate that the presence of RHA is delaying the formation of urea groups[63]. In this case, more isocyanate groups are available to react with polyol (Figure 11) procing C=O of ester associated with urethane (1700 cm^{-1}). The reaction of isocyanate with water gives rise to urea groups and carbon dioxide, which expands the foam (expansion reaction). During the experiments, it was observed that the expansion of PUF-RHA was slower than that of PUF-REF. Obviously the system is more viscous, but the formation of lesser urea also helps to retard the expansion. This occurs more markedly with PUF-RH than with PUF-CR.

The main FTIR bands of the polyurethane are given in Table 3[38,42,56,60-62,64]. The predominance of polyurethane bands are clear in both spectra of PUF composites (Figure 9 and Figure 10).

Figure 12 shows the results of the contact angle (CA) test for polyurethane foam and its composites. The data shows a hydrophobic characteristic of the PU-REF adsorbent ($\theta > 90°$), and its value is compatible with the literature[37,65].

After incorporating RHA into the polymer, the contact angle increased, making the material's hydrophobicity more evident. Incorporating CR into PU reduced its contact angle. Incorporating CR into PU reduced its contact angle,

likely due to the high surface area and pore size seen in silica-based adsorbents[17]. Studies indicate that hydrophobic surfaces are highly suitable for the adsorption of organic components[1,25,65,66].

3.3. Calibration curve

Figure 13 shows the absorption spectra of the pesticides in solutions with concentrations ranging from 5 to 500 mg/L, analyzed in the 185 to 400 nm range. The maximum absorbance peak was observed at wavelengths of 283 nm

Table 3. The main characteristic FTIR bands of the polyurethanes.

Wavelenghth (cm^{-1})	Assignment[a]
3295	st N-H
2930 - 2862	st C-H (CH$_2$) asym and sy respectively
2260	st N=C=O
1717	st C=O (ester and urethane-associated)
1600	st sy COO
1523	st C-N and δ N-H
1450	δ CH$_2$ and δ CH$_3$
1370	δ_{oop} C-H (CH$_2$)
1236	st asy N-CO-O and st C-O-C
1100	st C-O-C
1043	st sy N-CO-O and st C-O-C
995	st C-O-C

[a]st: stretching, δ: bending, sy; symmetric, asym: non-symmetric, δ_{oop}: bending out the plane.
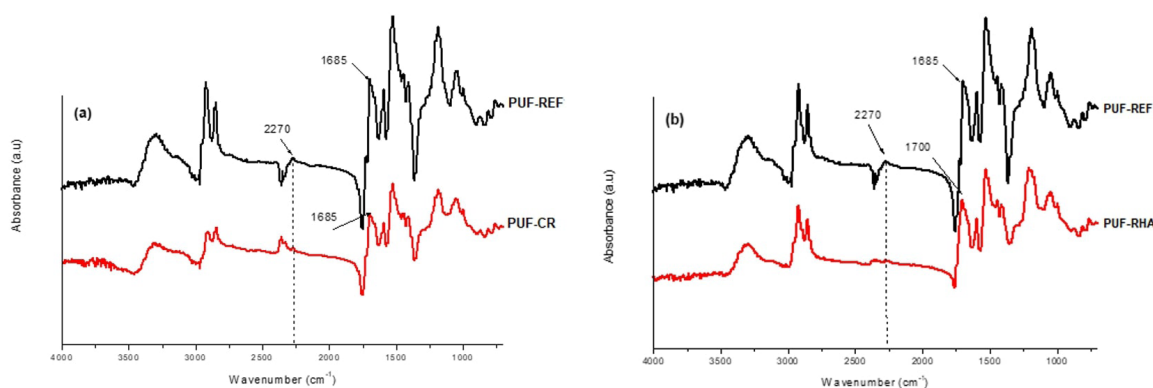

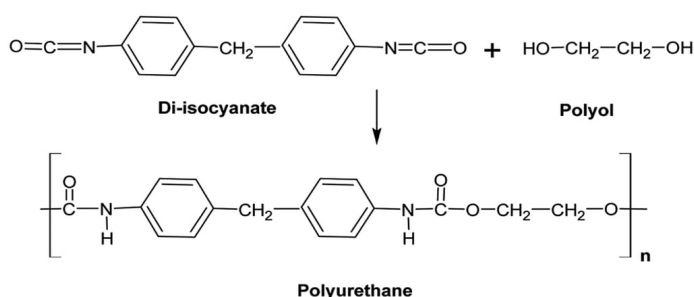**Figure 10.** FTIR spectra of PUF-REF and PUF-CR (a), PUF-REF and PUF-RHA (b).

Figure 11. Polyurethane synthesis reaction through the reaction between diisocyanate and polyol[62].

for 2,4-D (Figure 13a), 279 nm for mancozeb (Figure 13b) and 193 nm for glyphosate (Figure 13c)[45-47]. Analysis of the control sample confirmed the absence of adsorption of the pesticides on the glass surfaces during the calibration process and/or measurements.

3.4. Adsorption study as a function of pesticide concentration

First, the results of control experiments demonstrated that there was no degradation of any of the three pesticides—glyphosate, mancozeb, and 2, 4-D under the conditions of the present study. This is consistent with previous studies in which the adsorption of mancozeb and 2,4-D was evaluated over pH ranges of 3 to 11[46] and 2 to 10[67], respectively, while glyphosate was tested over a range from 2 to 10[68].

All adsorbents developed in this study (PU-REF, PU-RHA, and PU-CR) were evaluated in adsorption tests for the pesticides 2,4-D, mancozeb, and glyphosate, using concentrations of 50 mg/L and 300 mg/L and pH 7. In the adsorption test for the pesticide 2,4-D (Figure 14a), removal was recorded at all the concentrations studied (50 mg/|L and 300 mg/L), ranging from 0.11 mg/g (1.27%) to 2.02 mg/g (4.33%), respectively. On the other hand, for mancozeb (Figure 14b), significant removal was observed at high concentrations (300 mg/L) with a value of 12.78 mg/g (24.90%), for the composite containing petrochemical residue. With regard to glyphosate (Figure 14c), there was no detectable adsorption at the concentrations tested with the synthesized adsorbents. For the polymer composite incorporated with rice husk ash, there was no adsorption for the pesticides glyphosate and 2,4-D.
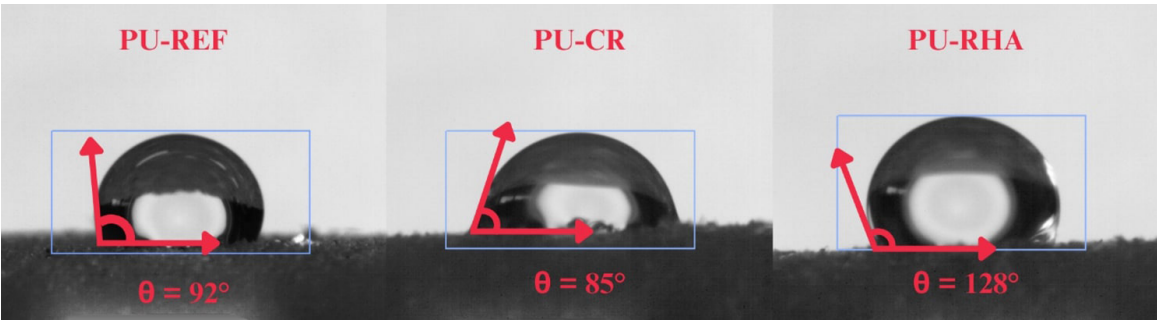

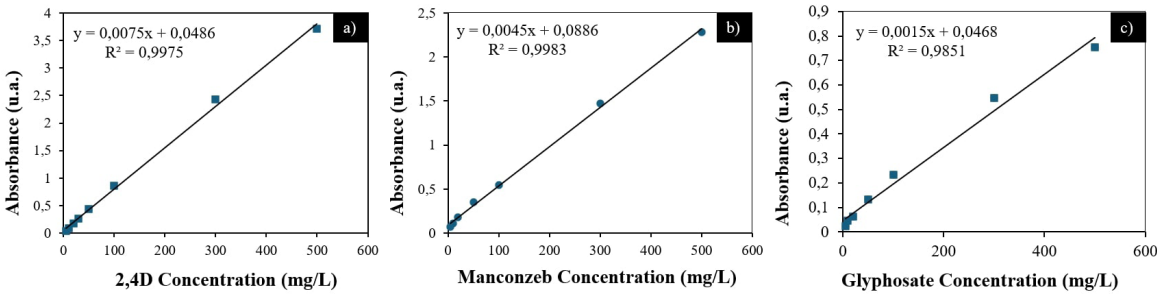**Figure 12.** Contact angle of synthesized foams.

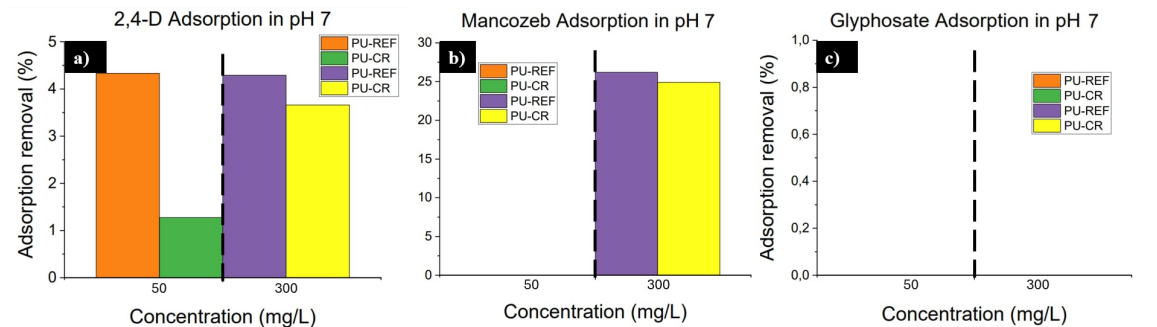**Figure 13.** Calibration curves of 2,4-D (a), Mancozeb (b) and Glyphosate (c).

Figure 14. Adsorption of pesticides using PU foams and composites at pH 7: a) 2,4-D, b) Manconzeb and c) Glyphosate.

Innovative Polyurethane Foam from Agro-Industrial and Petrochemical Waste: A Sustainable Solution for
Adsorbing Organic Pollutants in Natural Waters

11

For the pesticide mancozeb, the adsorption efficiency was extremely low. Other organic and inorganic contaminants should be investigated with polyurethane foams incorporating rice husk ash to evaluate their adsorption potential for a wider range of pollutants.

3.5. Adsorption study as a function of pH variation

The pH of the solution is crucial in the aqueous environment as it significantly influences the adsorption performance of the adsorbent[64]. In the study, for 2,4-D, adsorption was ~ 4% (2.10 mg/g) for the foam containing petroleum catalyst residue at a concentration of 300 mg/L at pH = 2, while at pH = 12 no adsorption was observed (Figures 15a and 15b). Mancozeb showed a substantial increase in removal efficiency with the incorporation of catalyst residue, reaching approximately 100% (17.97 mg/g) and 98% (45.98 mg/g) removal at pH 2 for concentrations of 50 mg/L and 300 mg/L, respectively (Figure 15c). These values are higher than those reported in the literature for some organic contaminants in aqueous systems, such as methylene blue (93.75%)[69] and textile effluents (47.86%)[70]. In the aqueous solution at pH = 12, visual changes in color and turbidity were noticed, altering the behavior of the UV-vis curve and suggesting a possible reaction with NaOH. For glyphosate, no adsorption was observed at pHs 2 and 12. All the composites synthesized with the incorporation of rice husk ash, PU-RHA, showed lower removal efficiency compared to the composites containing catalyst residue, with the highest removal percentages for mancozeb of (62.5% for pH 2 and 47.3% for pH 12 at a concentration of 300 mg/L, Figures 15c, 15d). For an aqueous system with a concentration of 50 mg/L, the adsorption efficiencies were 45% for pH 2 (Figure 15c) and 34% for pH 12 (Figure 15d).

The polymer composites did not show adsorption for glyphosate and 2,4-D (Figures 15e, 15f).

Most of the time, as the initial concentration increases, there is a decrease in absorption capacity. Initial concentration of the adsorbate in the solution creates the driving force (concentration gradient) for mass transfer between the solution and the adsorbent[71]. At lower concentration, the ratio of the number of solute molecules to the adsorbent surface is low. At high concentrations, however, the ratio becomes high i.e. the unused adsorption sites for adsorbate decrease and the adsorption uptake capacity depends on the initial concentration[71]. This matches with many studies in which removal percentages showed a decreasing trend with increasing concentration[46]. The authours attributed this to the increased numbers of mancozeb molecules (adsorvate) than the numbers of active sites of biochar (adsorbent). The increase in removal efficiency at higher concentrations may seem counterintuitive, since progressive saturation of active sites is expected. This little expected behavior might be explained by the higher concentration gradient, which acts as a stronger driving force for mass transfer of the contaminant from the solution to the adsorvent. Similar results have also been reported in literature using polyurethane-based adsorbents, suggesting that this behavior may be a characteristic feature of such materials[1,42]. This hypothesis should be tested in further studies exploring higher concentration ranges.

The results of the control experiment demonstrated that there was no degradation of any of the three pesticides—glyphosate, mancozeb, and 2,4-D—analyzed individually under the evaluated conditions, confirming their stability in the aqueous system throughout the study period.

The point of zero charge (PZC) for each sample provides understanding of how adsorbents interact with the adsorbate at different pH levels of the solution (Jankowska et al., 2024).
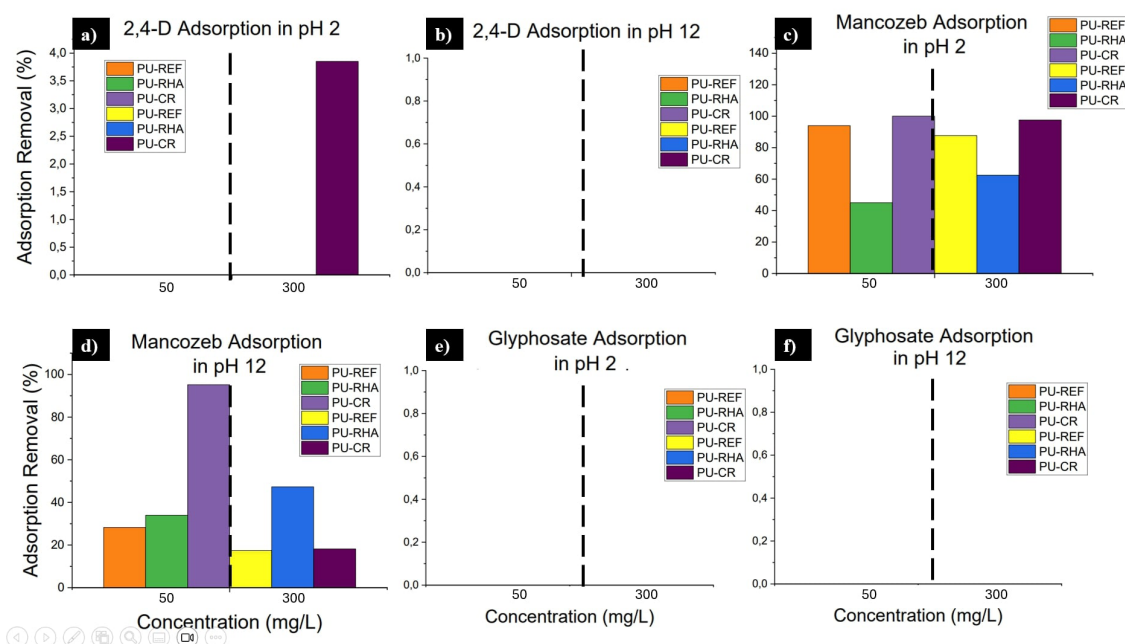

Figure 15. Adsorption tests with pH variation.

Zeta potential measurements were performed and found PZC for RC and PUF as 2.55 and 6.05, respectively[1]. The PZC 8.3 of RHA was determined by others using the solid addition method[72]. The pKa of 2, 4-D and glyphosate were reported as 2.8[73] and 2.6[68], respectively. Mancozeb does not have a specific pKa value, as it is a complex chemical compound and not a simple substance with a single acidic functional group. Despite this, an average pKa value of 10.3 for mancozeb has been considered[46]. It is well known that, the adsorbent surface is positively charged at pH lower than its PZC, and negatively charged at pH lower than its pzc. On the other hand, the adsorbate exists in the cationic form at pH lower than its pKa and anionic form at pH higher than its pKa (Jankowska et al.[73]). Therefore, electrostatic attraction between adsorbents and adsorbates tends to occur when the charges are opposite, leading to the most effective removal of pollutants. In order to estimate the sole pH effect in the total removal efficiency. According to the literature, the pH effect is negligible for most systems that have been tested.

3.6. Influence of contact time on the adsorption performance of mancozeb

Due to the high removal efficiency observed when the adsorbents were exposed to the mancozeb solution (300 mg/L), a study of the adsorption kinetics of this pesticide was carried out for contact times ranging from 0.5 to 44 hours. Figure 16 shows the influence of contact time on mancozeb removal efficiency at pH 2, using the foams developed. The amount of pesticide adsorbed increased with contact time and the adsorption capacity rapidly increases during the first 1.0 h of the contact. This rapid initial adsorption can be attributed to the immediate availability of active sites in the foams. The highest values were reached in 24 h, subsequently the adsorption capacity decreased until reaching saturation (not shown). The order of maximum removal percentages shown in Figure 16 might be affected by the average pore size of the adsorvents[74]. Smaller pores can lead to higher adsorption capacity due to increased surface area and stronger interactions, such as in PU-CR with average pore size of 294 μm. Larger pores facilitate the diffusion, but have lower surface area and weaker interactions, such as in PU-RHA with average pore size of 806 μm. On the other hand, the adsorption capacity of PU-REF, with average pore size of 656 μm, presented an intermediary adsorption capacity. Researchers[46] used biochar produced from neem chip for removing mancozeb from wastewater. Fixing the contact time at 24 h, they found 78.54% for removal percentage (c_i= 300 mg·L-1 and pH=5.0). In the study, the highest values can be observed for the maximal experiment time of 24 h, which vary between 85% (PU- REF) and 98% (PU-CR).

Mechanical properties of the foams, such as compressive strength and elasticity, are indeed crucial for practical applications, particularly in ensuring the material's integrity during repeated adsorption–desorption cycles. Although mechanical testing was not the focus of the present study, the cyclic stress–strain curves provide an initial indication of the foam's elastic recovery ability. High mechanical stability is essential to maintain adsorption performance over multiple squeezing cycles, which directly impacts the reusability and long-term applicability of the material[75]. However, the
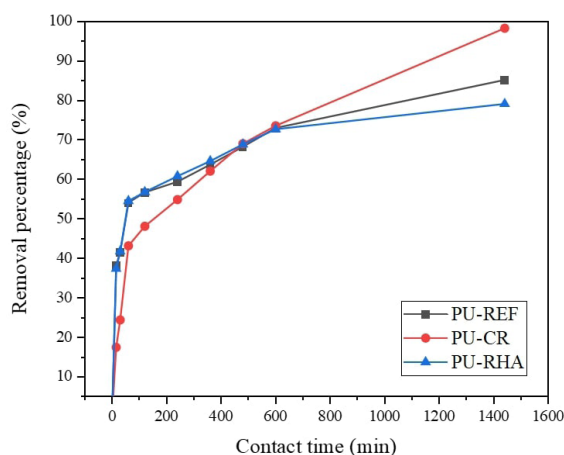

Figure 16. Effect of contact time with initial concentrations of 300 mg·L⁻¹ (and aqueous solution with pH 2) on mancozeb removal efficiency.

primary objective of this work was to identify an efficient and feasible adsorbent–adsorbate system. Future studies will include reuse experiments and detailed mechanical characterization to further assess the practical viability of the proposed material. It is also worth noting that similar studies in the literature focused on adsorption performance without reporting mechanical test results[76,77].

Although desorption and reusability experiments were not the focus of this study, these aspects have been previously investigated, with studies demonstrating that polyurethane foam can be successfully regenerated and reused for at least three adsorption–desorption cycles without significant loss of performance or saturation[1].

4. Conclusion

Bio-based polyurethane foams from castor oil with petrochemical and agro-industrial waste were developed and extensively characterized to be evaluated as adsorbents of organic contaminants in natural waters. Scanning electron microscopy and microtomography characterizations demonstrated that the prepared adsorbents exhibit high porosity and significant interconnectivity between pores, which may favor the removal of organic contaminants in water. The contact angle results indicated a hydrophobic behavior of the foams and this behavior favors adsorption. Was observed that the foams did not show significant adsorption for the pesticide glyphosate and 2,4 - D, regardless of the pH variations. At pH 2 and 300 mg/L, PU-RHA foams showed lower mancozeb removal 62.5% (29.87 mg/g) compared to PU-CR and the control foam (PU-REF) which reached 98% (45.98 mg/g) and 85% (38.60 mg/g), respectively. These results offer new perspectives for optimizing the adsorption of organic contaminants in sustainable bio-based polyurethane foams, comprises waste reduction, reuse and recycling promoting advances in sustainability and the circular economy. The feasibility of developing affordable and effective solutions for water treatment can benefit communities, improve public health and reduce costs associated with treating contaminated water.

Innovative Polyurethane Foam from Agro-Industrial and Petrochemical Waste: A Sustainable Solution for
Adsorbing Organic Pollutants in Natural Waters

13

5. Acknowledgments

6. References

1. Almeida MLB, Ayres E, Libânio M, Gamarano DS, Ribeiro CC, Oréfice RL. Bio-based polyurethane foams with enriched surfaces of petroleum catalyst residues as adsorbents of organic pollutants in aqueous solutions. J Polym Environ. 2020;28(9):2511-22. http://doi.org/10.1007/s10924-020-01794-9.

2. Panis C, Candiotto LZP, Gaboardi SC, Gurzenda S, Cruz J, Castro M, et al. Widespread pesticide contamination of drinking water and impact on cancer risk in Brazil. Environ Int. 2022;165:107321. http://doi.org/10.1016/j.envint.2022.107321.

3. Rasheed T. Magnetic nanomaterials: greener and sustainable alternatives for the adsorption of hazardous environmental contaminants. J Clean Prod. 2022;362:132338. http://doi.org/10.1016/j.jclepro.2022.132338.

4. Ahamad T, Naushad M, Alshehri SM. Fabrication of magnetic polymeric resin for the removal of toxic metals from aqueous medium: kinetics and adsorption mechanisms. J Water Process Eng. 2020;36:101284. http://doi.org/10.1016/j.jwpe.2020.101284.

5. Sajid M, Asif M, Baig N, Kabeer M, Ihsanullah I, Mohammad AW. Carbon nanotubes-based adsorbents: Properties, functionalization, interaction mechanisms, and applications in water purification. J Water Process Eng. 2022;47:102815. http://doi.org/10.1016/j.jwpe.2022.102815.

6. Sivaranjanee R, Kumar PS. A review on cleaner approach for effective separation of toxic pollutants from wastewater using carbon spheres as adsorbent: Preparation, activation and applications. J Clean Prod. 2021;291:125911. http://doi.org/10.1016/j.jclepro.2021.125911.

7. Brasil. Conselho Nacional do Meio Ambiente. Resolução CONAMA nº 357/2005. Dispõe sobre a classificação dos corpos de água e diretrizes ambientais para o seu enquadramento, bem como estabelece as condições e padrões de lançamento de efluentes, e dá outras providências. Diário Oficial da União; Brasília; 17 mar. 2005.

8. Brasil. Instituto Brasileiro do Meio Ambiente e dos Recursos Naturais Renováveis [homepage on the Internet]. Relatórios e comercialização de agrotóxicos. Brasília: IBAMA; 2023 [cited 2023 Feb 21]. Available from: https://www.gov.br/ibama/pt-br/assuntos/quimicos-e-biologicos/agrotoxicos/relatorios-de-comercializacao-de-agrotoxicos

9. Richmond ME. Glyphosate: a review of its global use, environmental impact, and potential health effects on humans and other species. J Environ Stud Sci. 2018;8(3):416-34. http://doi.org/10.1007/s13412-018-0517-2.

10. Van Bruggen AHC, He MM, Shin K, Mai V, Jeong KC, Finckh MR, et al. Environmental and health effects of the herbicide glyphosate. Sci Total Environ. 2018;616–617:255-68. http://doi.org/10.1016/j.scitotenv.2017.10.309.

11. Dall'Agnol JC, Pezzini MF, Uribe NS, Joveleviths D. Systemic effects of the pesticide mancozeb : a literature review. Eur Rev Med Pharmacol Sci. 2021;25(11):4113-20. http://doi.org/10.26355/eurrev_202106_26054.

12. Islam F, Wang J, Farooq MA, Khan MSS, Xu L, Zhu J, et al. Potential impact of the herbicide 2,4-dichlorophenoxyacetic acid on human and ecosystems. Environ Int. 2018;111:332-51. http://doi.org/10.1016/j.envint.2017.10.020.

13. Dalsager L, Christensen LE, Kongsholm MG, Kyhl HB, Nielsen F, Schoeters G, et al. Associations of maternal exposure to organophosphate and pyrethroid insecticides and the herbicide 2,4-D with birth outcomes and anogenital distance at 3 months in the Odense Child Cohort. Reprod Toxicol. 2018;76:53-62. http://doi.org/10.1016/j.reprotox.2017.12.008.

14. Buledi JA, Mahar N, Mallah A, Solangi AR, Palabiyik IM, Qambrani N, et al. Electrochemical quantification of mancozeb through tungsten oxide/reduced graphene oxide nanocomposite: a potential method for environmental remediation. Food Chem Toxicol. 2022;161:112843. http://doi.org/10.1016/j.fct.2022.112843.

15. Rasouli K, Rasouli J, Mohtaram MS, Sabbaghi S, Kamyab H, Moradi H, et al. Biomass-derived activated carbon nanocomposites for cleaner production: a review on aspects of photocatalytic pollutant degradation. J Clean Prod. 2023;419:138181. http://doi.org/10.1016/j.jclepro.2023.138181.

16. Jagadeesh N, Sundaram B. Adsorption of pollutants from wastewater by biochar: a review. J Hazard Mater Adv. 2023;9:100226. http://doi.org/10.1016/j.hazadv.2022.100226.

17. Ewis D, Hameed BH. A review on microwave-assisted synthesis of adsorbents and its application in the removal of water pollutants. J Water Process Eng. 2021;41:102006. http://doi.org/10.1016/j.jwpe.2021.102006.

18. Zeb S, Ali N, Ali Z, Bilal M, Adalat B, Hussain S, et al. Silica-based nanomaterials as designer adsorbents to mitigate emerging organic contaminants from water matrices. J Water Process Eng. 2020;38:101675. http://doi.org/10.1016/j.jwpe.2020.101675.

19. Hanafi MF, Sapawe N. A review on the current techniques and technologies of organic pollutants removal from water/wastewater. Mater Today Proc. 2021;31(6):A158-65. http://doi.org/10.1016/j.matpr.2021.01.265.

20. Chauhan PR, Baiju V, Asif Sha A, Tyagi SK. Adsorption of ethanol onto novel and indigenous green adsorbents: synthesis, characterization, and applications. J Clean Prod. 2024;442:140978. http://doi.org/10.1016/j.jclepro.2024.140978.

21. Wang H, Shan L, Lv Q, Cai S, Quan G, Yan J. Production of hierarchically porous carbon from natural biomass waste for efficient organic contaminants adsorption. J Clean Prod. 2020;263:121352. http://doi.org/10.1016/j.jclepro.2020.121352.

22. Rojas R, Vanderlinden E, Morillo J, Usero J, El Bakouri H. Characterization of sorption processes for the development of low-cost pesticide decontamination techniques. Sci Total Environ. 2014;488–489:124-35. http://doi.org/10.1016/j.scitotenv.2014.04.079.

23. Gomes HO, Freire PTC, Nascimento RF, Teixeira RNP. Removal of contaminants from water using *Moringa oleifera* Lam. as biosorbent: an overview of the last decade. J Water Process Eng. 2022;46:102576. http://doi.org/10.1016/j.jwpe.2022.102576.

24. Bo G, Jiao L, Li H, Zhao G, Xu Z, Liu X, et al. Effective removal of phenol from polluted water via bio-based rigid polyurethane foams in collaboration with Alcaligenes faecalis. J Water Process Eng. 2023;53:103876. http://doi.org/10.1016/j.jwpe.2023.103876.

25. Anfar Z, Ahsaine HA, Zbair M, Amedlous A, El Fakir AA, Jada A, et al. Recent trends on numerical investigations of response surface methodology for pollutants adsorption onto activated carbon materials: a review. Crit Rev Environ Sci Technol. 2019;50(10):1043-84. http://doi.org/10.1080/10643389.2019.1642835.

26. Li S, Lu J, Zhang T, Cao Y, Li J. Relationship between biochars' porosity and adsorption of three neutral herbicides from water. Water Sci Technol. 2017;75(2):482-9. http://doi.org/10.2166/wst.2016.535.

27. Ali I, Basheer AA, Mbianda XY, Burakov A, Galunin E, Burakova I, et al. Graphene-based adsorbents for remediation of noxious pollutants from wastewater. Environ Int. 2019;127:160-80. http://doi.org/10.1016/j.envint.2019.03.029.

28. Ali A, Alharbi OML, Tkachev A, Galunin E, Burakov A, Grachev VA. Water treatment by new-generation graphene materials: hope for bright future. Environ Sci Pollut Res Int. 2018;25(7):7315-29. http://doi.org/10.1007/s11356-018-1315-9.

29. Bano Z, Akram M, Ali NZ, Khan MU, Wang F, Li L, et al. Sustainable porous graphene/Co-MOF for the removal of water pollutants: combined theoretical and experimental studies. J Water Process Eng. 2024;59:104982. http://doi.org/10.1016/j.jwpe.2024.104982.

30. Ali I, Alharbi OML, Alothman ZA, Alwarthan A. Facile and eco-friendly synthesis of functionalized iron nanoparticles for cyanazine removal in water. Colloids Surf B Biointerfaces. 2018;171:606-13. http://doi.org/10.1016/j.colsurfb.2018.07.071.

31. Ali I, Alharbi OML, Alothman ZA, Badjah AY, Alwarthan A, Basheer AA. Artificial neural network modelling of amido black dye sorption on iron composite nanomaterial: kinetics and thermodynamics studies. J Mol Liq. 2018;250:1-8. http://doi.org/10.1016/j.molliq.2017.11.163.

32. Atasoy AD, Bilgic B. Adsorption of copper and zinc ions from aqueous solutions using montmorillonite and bauxite as low-cost adsorbents. Int J Mine Water. 2017;37:205-10. http://doi.org/10.1007/s10230-017-0464-2.

33. Vasiljević BN, Obradović M, Bogdanović DB, Milojević-Rakić M, Jovanović Z, Gavrilov N, et al. *In situ* synthesis of potassium tungstophosphate supported on BEA zeolite and perspective application for pesticide removal. J Environ Sci. 2019;81:136-47. http://doi.org/10.1016/j.jes.2019.01.018.

34. Hosseini N, Toosi MR. Removal of 2,4-D, glyphosate, trifluralin, and butachlor herbicides from water by polysulfone membranes mixed with graphene oxide/TiO_2 nanocomposite: study of filtration and batch adsorption. J Environ Health Sci Eng. 2019;17(1):247-58. http://doi.org/10.1007/s40201-019-00344-3.

35. Ali I, Alharbi OML, Alothman ZA, Badjah AY. Kinetics, thermodynamics, and modeling of Amido Black dye photodegradation in water using Co/TiO_2 nanoparticles. Photochem Photobiol. 2018;94(5):935-41. http://doi.org/10.1111/php.12937.

36. Almeida MLB, Ayres E, Moura FCC, Orefice RL. Polyurethane foams containing residues of petroleum industry catalysts as recoverable pH-sensitive sorbents for aqueous pesticides. J Hazard Mater. 2018;346:285-95. http://doi.org/10.1016/j.jhazmat.2017.12.033.

37. Zimmermann MVG, Zattera AJ, Fenner BR, Santana RMC. Sorbent system based on organosilane-coated polyurethane foam for oil spill clean up. Polym Bull. 2021;78(1–2):1423-40. http://doi.org/10.1007/s00289-020-03169-5.

38. Zhang J, Wu S, Zhang K, Li C, Ling G, Ji C, et al. Novel polyurethane viscoelastic foam modified with discarded luffa seed oil in accordance with cleaner production. J Clean Prod. 2022;341:130795. http://doi.org/10.1016/j.jclepro.2022.130795.

39. Akindoyo JO, Beg MDH, Ghazali S, Islam MR, Jeyaratnam N, Yuvaraj AR. Polyurethane types, synthesis and applications – a review. RSC Advances. 2016;6(115):114453-82. http://doi.org/10.1039/C6RA14525F.

40. Barroso-Solares S, Merillas B, Cimavilla-Román P, Rodriguez-Perez MA, Pinto J. Enhanced nitrates-polluted water remediation by polyurethane/sepiolite cellular nanocomposites. J Clean Prod. 2020;254:120038. http://doi.org/10.1016/j.jclepro.2020.120038.

41. Jiang H, Zhang Z, Lin Z, Gong X, Guo H, Wang H. Modification of polyurethane sponge filler using medical stones and application in a moving bed biofilm reactor for ex situ remediation of polluted rivers. J Water Process Eng. 2021;42:102189. http://doi.org/10.1016/j.jwpe.2021.102189.

42. Pereira MVV, Nunes EHM, Couto C, Ayres E, Orefice RL, Libânio M, et al. Eco-friendly polyurethane composites with rice husk ash residue to remove petroleum hydrocarbons from aqueous media. Polym Bull. 2024;81(13):11773-94. http://doi.org/10.1007/s00289-024-05255-4.

43. Endale SA, Taffese WZT, Vo D, Yehualaw MD. Rice husk ash in concrete. Sustainability. 2022;15(1):125960. http://doi.org/10.3390/su15010137.

44. Oliveira DM, Agostinetto L, Siegloch AE. Comparison of the drinking water standard for pesticides of Brazil with other countries. Heliyon. 2023;9(3):e13783. http://doi.org/10.1016/j.heliyon.2023.e13783.

45. Páez MR, Ochoa-Muñoz Y, Rodriguez-Páez JE. Efficient removal of a glyphosate-based herbicide from water using ZnO nanoparticles (ZnO-NPs). Biocatal Agric Biotechnol. 2019;22:101434. http://doi.org/10.1016/j.bcab.2019.101434.

46. Manoharan T, Ganeshalingam S, Nadarajah K. Mechanisms of emerging contaminants removal by novel neem chip biochar. Environ Adv. 2022;7:100158. http://doi.org/10.1016/j.envadv.2021.100158.

47. Girón-Navarro R, Martínez-Miranda V, Teutli-Sequeira A, Linares-Hernández I, Martínez-Cienfuegos I, Sánchez Pozos M, et al. A solar photo-Fenton process with calcium peroxide from eggshell and ferrioxalate complexes for the degradation of the commercial herbicide 2,4-D in water. J Photochem Photobiol Chem. 2023;438(2):114550. http://doi.org/10.1016/j.jphotochem.2023.114550.

48. Bardestani R, Roy C, Kaliaguine S. The effect of biochar mild air oxidation on the optimization of lead (II) adsorption from wastewater. J Environ Manage. 2019;240:404-20. http://doi.org/10.1016/j.jenvman.2019.03.110.

49. Kaur G, Singh N, Rajor A, Arya RK. Removal of doxycycline hydrochloride from aqueous solution by rice husk ash using response surface methodology and disposability study. Environ Sci Pollut Res Int. 2022;30(1):8485-99. http://doi.org/10.1007/s11356-022-18961-1.

50. Lataye D, Mishra I, Mall ID. Pyridine sorption from aqueous solution by rice husk ash (RHA) and granular activated carbon (GAC): parametric, kinetic, equilibrium and thermodynamic aspects. J Hazard Mater. 2008;154(1–3):858-70. http://doi.org/10.1016/j.jhazmat.2007.10.111.

51. Payá J, Monzó J, Borrachero MV. Physical, chemical and mechanical properties of fluid catalytic cracking catalyst residue (FC3R) blended cements. Cement Concr Res. 2001;31(1):57-61. http://doi.org/10.1016/S0008-8846(00)00432-4.

52. Mohammadi A, Salehi E, Aghazadeh H, Ramezani A, Eidi B. An efficient method for recycling spent residue cat-cracking catalysts (SRC) to prepare broadly-applicable mullite-based wear-resistant ceramics. Appl Clay Sci. 2020;187:105488. http://doi.org/10.1016/j.clay.2020.105488.

53. Madhu J, Santhanam A, Natarajan M, Velauthapillai D. CO2 adsorption performance of template free zeolite A and X synthesized from rice husk ash as silicon source. RSC Advances. 2022;12(36):1-19. http://doi.org/10.1039/D2RA04052B.

54. Fooladgar S, Teimouri A, Ghanavati Nasab S. Highly efficient removal of lead ions from aqueous solutions using chitosan/rice husk ash/nano alumina with a focus on optimization by response surface methodology: isotherm, kinetic, and thermodynamic studies. J Polym Environ. 2019;27(4):1025-42. http://doi.org/10.1007/s10924-019-01385-3.

55. Bakdash RS, Aljundi IH, Basheer C, Abdulazeez I. Rice husk derived Aminated Silica for the efficient adsorption of different gases. Sci Rep. 2020;10(1):19526. http://doi.org/10.1038/s41598-020-76460-0.

56. Xu M, Pan G, Guo Y, Liang Q, Yu Z, Cao Y, et al. Highly efficient oil-water separation and oil adsorption with hydrophobic hydrotalcite/polyurethane porous composite foam. J Water Process Eng. 2024;60:105211. http://doi.org/10.1016/j.jwpe.2024.105211.

57. Ewis D, Hameed BH. A review on microwave-assisted synthesis of adsorbents and its application in the removal of water pollutants. J Water Process Eng. 2021;41:102006. http://doi.org/10.1016/j.jwpe.2021.102006.

58. Kahlerras Z, Irinislimane R, Bruzaud S, Belhaneche-Bensemra N. Elaboration and characterization of polyurethane foams based on renewably sourced polyols. J Polym Environ. 2020;28(3):3003-18. http://doi.org/10.1007/s10924-020-01833-5.

59. Lu J, Liao C, Cheng L, Jia P, Yin Z, Song L, et al. Cleaner production to a multifunctional polyurethane sponge with high fire safety and low toxicity release. J Clean Prod. 2022;333:130172. http://doi.org/10.1016/j.jclepro.2021.130172.

60. Costa JAS, Paranhos CM. Systematic evaluation of amorphous silica production from rice husk ashes. J Clean Prod. 2018;192:688-97. http://doi.org/10.1016/j.jclepro.2018.05.028.

61. Gendron-Badou A, Coradin T, Maquet J, Fröhlich F, Livage J. Spectroscopic characterization of biogenic silica. J Non-Cryst Solids. 2003;316(2-3):331-7. http://doi.org/10.1016/S0022-3093(02)01634-4.

Innovative Polyurethane Foam from Agro-Industrial and Petrochemical Waste: A Sustainable Solution for
Adsorbing Organic Pollutants in Natural Waters

15

62. Afonso TF, Demarco CF, Schoeler GP, Giongo JL, Vaucher RA, Cadaval TRS Jr, et al. Polyurethane foams incorporated with different fillers to remove SARS-CoV-2 from water. J Water Process Eng. 2023;54:104000. http://doi.org/10.1016/j.jwpe.2023.104000.

63. Vislohuzova T, Rozhnova R, Galatenko N. Development and research of polyurethane foam composite materials with albucid. Amer J Polym Sc Tech. 2021;7(3):38-43. http://doi.org/10.11648/j.ajpst.20210703.11.

64. Chen X, Cai D, Yang Y, Sun Y, Wang B, Yao Z, et al. Pyrolysis kinetics of bio-based polyurethane: evaluating the kinetic parameters, thermodynamic parameters, and complementary product gas analysis using TG/FTIR and TG/GC-MS. Renew Energy. 2023;205:490-8. http://doi.org/10.1016/j.renene.2023.01.078.

65. Ng ZC, Roslan RA, Lau WJ, Gürsoy M, Karaman M, Jullok N, et al. A green approach to modify surface properties of polyurethane foam for enhanced oil absorption. Polymers. 2020;12(9):1883. http://doi.org/10.3390/polym12091883.

66. Li N, Huo L, Shen W, Qiang C, Wu M, Sun G, et al. Porous organic polymers for superefficient removal of pollutants from water: Design, synthesis and adsorption performance. J Clean Prod. 2023;396:136558. http://doi.org/10.1016/j.jclepro.2023.136558.

67. Alaysuy O, Aljohani MM, Alkhamis K, Alatawi NM, Almotairy AR, Al-Ola KAA, et al. Synthesis, characterization and adsorption optimization of bimetallic La–Zn metal organic framework for removal of 2, 4-dichlorophenylacetic acid. Heliyon. 2024;10(7):e28622. http://doi.org/10.1016/j.heliyon.2024.e28622.

68. Bezerra WFDP, Dognani G, Alencar LND, Parizi MPS, Boina RF, Cabrera FC, et al. Chemical treatment of sugarcane bagasse and its influence on glyphosate adsorption. Materia. 2022;27(1):e13142. http://doi.org/10.1590/s1517-707620220001.1342.

69. Vonnie JM, Li CS, Erna KH, Yin KW, Felicia WXL, Aqilah MNN, et al. Development of eggshell-based orange peel activated carbon film for synergetic adsorption of cadmium (II) Ion. Nanomaterials. 2022;12(16):2750. http://doi.org/10.3390/nano12162750.

70. Gonçalves IL, Menezes FCM Fo, Morais EB, Castro VA, Canales FA. Optimization of the use of Moringa oleifera in wastewater treatment by rotational central composite design. Desalination Water Treat. 2024;320:100765. http://doi.org/10.1016/j.dwt.2024.100765.

71. Rathi BS, Kumar PS. Application of adsorption process for effective removal of emerging contaminants from water and wastewater. Environ Pollut. 2021;280:116995. http://doi.org/10.1016/j.envpol.2021.116995.

72. Srivastava VC, Mall ID, Mishra IM. Characterization of mesoporous rice husk ash (RHA) and adsorption kinetics of metal ions from aqueous solution onto RHA. J Hazard Mater. 2006;134(1-3):257-67. http://doi.org/10.1016/j.jhazmat.2005.11.052.

73. Jankowska A, Panek R, Franus W, Goscianska J. Tailoring natural and fly ash-based zeolites surfaces for efficient 2, 4-D herbicide adsorption: the role of hexadecyltrimethylammonium bromide modification. Molecules. 2024;29(22):5244. http://doi.org/10.3390/molecules29225244.

74. Hsieh CT, Teng H. Influence of mesopore volume and adsorbate size on adsorption capacities of activated carbons in aqueous solutions. Carbon. 2000;38(6):863-9. http://doi.org/10.1016/S0008-6223(99)00180-3.

75. Li X, Zhang J, Liu H, Li Z, Zheng G, Zhou L, et al. Sustainable superhydrophobic lignin-based polyurethane foam: an innovative solution for oil pollutant adsorption. RSC Advances. 2025;15(1):377-87. http://doi.org/10.1039/D4RA07384C.

76. Merillas B, Rodríguez-Pérez MÁ, Durães L. Enhanced copper-adsorption removal from water by easy-handling silica aerogel-polyurethane foam composites. J Ind Eng Chem. 2025;146:578-88. http://doi.org/10.1016/j.jiec.2024.11.041.

77. Singh KK, Goel NK, Kanjilal A, Ruhela R, Kumar V, Bhattacharyya K, et al. Radiation grafted polyacrylic acid–polyurethane foam copolymer for efficient toxic metal removal from aqueous waste: a sustainable approach to waste management. Polym Bull. 2024;81(15):13435-60. http://doi.org/10.1007/s00289-024-05340-8.

Data availability

Data will be made available on request.